Journal of the Korean Nuclear Society
Volume 29, Number 2, pp. 110~126, April 1997

Development and Application of Two-Dimensional Hydrogen Mixing Model in Containment Subcompartment Under Severe Accidents

Byung-Chul Lee,* Jae-Seon Cho, Goon-Cherl Park, and Chang-Hyun Chung
Seoul National University
San 56-1, Shinlim-dong, Kwanak-gu, Seoul 151-742, Korea

(Received May 6, 1996)

Abstract

A two-dimensional continuum model for the hydrogen mixing phenomena in the containment subcompartment under severe accident conditions has been developed to predict the spatial distribution of the hydrogen concentration. The model can predict the distribution of time-dependent hydrogen concentration for HEDL experiments well. For the simulation of these experiments, the hydrogen is mixed uniform within the test compartment. To predict the extent of non-uniform distribution, the dominant factors such as the geometrical shape of obstacle and velocity of source injection in mixing phenomena are investigated. If the obstacle disturbing the flow of gas mixture exists in the compartment, the uniform distribution of hydrogen might be not guaranteed. The convective circulation of gas flow is separately formed up and down of the obstacle position, which makes a difference of hydrogen concentration between the upper and lower region of the compartment. The recirculation flow must have a considerable mass flow rate relative to velocity of the source injection to sustain the well-mixed conditions of hydrogen. Finally, in order to account for non-uniform distribution of the hydrogen due to the geometrical configuration the maximum-to-average ratio is functionalized.

1. Introduction

The hydrogen burn of TMI-2 accident fostered renewed attention to the issue of the impact of hydrogen on the reactor safety. There are many important aspects of this problem, and a lot of works have been performed in this area over the past decade. In general, hydrogen phenomena can be divided into four categories: generation and source injection, prechemical reaction transport, chemical reaction (detonation or deflagration), and control strategies. Among these categories, this study will focus on prechemical reaction transport in order to predict the distribution of hydrogen concentration under severe accident conditions.

The mixing transient of hydrogen can be affected by numerous mixing mechanism, including source momentum, forced convection, inter-compartmental pressure gradient driven flow, natural convection and diffusion as shown in Table 1. These physical intuition must be translated into mathematical expressions for problems to be addressed in a tractable form. Most analytical models[1~7] can be broadly grouped into two categories, lumped-parameter mod-

*Current Address: Korea Power Engineering Company, Inc.

els and continuum models. The computer codes, CONTAIN, MARCH, or MAAP which have been generally used to calculate the hydrogen mixing in containment during severe accidents use a lumped parameter model based on control volume or nodal balances of passive entities such as component mass and energy. These model provide accurate descriptions for large uniformly mixed volumes. However, the underlying assumption is that of well-mixed volumes, which no spatial details within a compartment can be described.

Table 1. Important Hydrogen Mixing Mechanisims

Mechanism	Description
Source momentum	Especially entrainment caused by strong jets
Intercompar tmental flow	Driven by pressure gradients produced by heterogeneous sources and localized heat mass transfer
Forced convection	Produced by mechanical devices, such as recirculation fans and fan coolers, and by momentum transfer from sprays.
Natural convection	Buoyant flows induced by source gases, temperature differences, heat transfer to cold sinks, and condensation ; affected by initial compartment conditions.
Diffusion	Both molecular and turbulent

On the other hand, the continuum category itself includes different physical models ranging from multiphase compressible treatments to single-phase homogeneous incompressible flow. Some computer codes include more than one of these treatments. In addition to the mass, energy, and momentum balances, other physical relationship must be included to close the analytical models. The requirements of model to be considered are summarized in Table 2.

The post-TMI actions had determined the installation of new mitigative systems in the smaller volume or more compartmentalized spaces, which emphasized that there is a possibility that the local hydrogen concentration may be increased to a level of unpredicted high. If the obstacle disturbing the flow of hydrogen concentration exists within the subcompartment, the peak concentration of the hydro-

Table 2. Analytical Model Characteristics

Mass, Momentum, and Energy Conservation Models
Lumped parameter : nodal balance augmented by internodal flow.
Multiphase compressible continuum : two phase, heterogeneous slip flow with numerous components and interphasic exchange
Single-phase compressible continuum : complete momentum and energy coupling, pressure-wave progpagation, and flow work important.
Incompressible continuum : momentum and energy balances decoupled by using Boussinesq approximation ; small compressibility allowed.
Ancillary Models
Thermodynamics : mixture dynamics, phase change.
Physical propertise : mixture formulas.
Transport mechanisms : turbulence modeling, multicomponent diffusion.
Equipment models : fans,sprays,coolers, structures.
Heat sinks : heat/mass transfer models, transient conduction
Numerical Solution
Accuracy
Versatility
Computational efficiency

gen can deviate from the allowed its range, and thus may bring about unexpected hydrogen burning in local region. Therefore, to quantify the non-uniform distribution of the hydrogen precisely and to provide the guideline for establishing the control strategy such as the installation of the igniter at the predicted spot showing high local concentration of the hydrogen, a more accurate model to predict the hydrogen transport in subcompartment is needed.

In this study, a two-dimensional axi-symmetric continuum model will be developed. For a source of high velocity, the source momentum is transferred by turbulent mixing model. The flow agitation by fan can make the driving force added to guarantee the uniform distribution of the hydrogen concentration. The calculation result will be compared with data of the experiment performed under severe accident conditions. And to analyze the non-uniform distribution of the hydrogen, the obstacle will be installed in various forms within the test compartment. From these analyses, the local agglomeration of the hydrogen concentration will be confirmed. Finally, the dominant physical factors affecting the hydrogen distribution within test compartment will be investigated to provide a basis on making the functionalized maximum-to-average ratio. This ratio will support the lumped parameter code's calculation and the establishment of the hydrogen control strategies.

2. The Development of Analytical Model

A two-dimensional incompressible continuum model is established by treating one velocity field of the mixture of multi-fluid such as hydrogen(or helium), steam, and air. The velocity of mixture is defined by,

$$v = \frac{\sum_{i=1}^{N} \rho_i V_i}{\sum_{i=1}^{N} \rho_i} \tag{1}$$

for a mixture of N species. The independent behavior of gas species is treated by the equation of species continuity.

The governing equations for a analytical model expressed in two-dimensional cylindrical coordinate are given as;

−Continuity Equation

$$\frac{\partial \rho}{\partial t} + \frac{1}{r}\frac{\partial}{\partial r}(\rho r u_r) + \frac{\partial}{\partial z}(\rho u_z) = 0 \tag{2}$$

−Momentum Equation

−r-component

$$\rho\left(\frac{\partial u_r}{\partial t} + u_r\frac{\partial u_r}{\partial r} + u_z\frac{\partial u_r}{\partial z}\right) = -\frac{\partial P}{\partial r} + \mu\left[\frac{\partial}{\partial r}\left(\frac{1}{r}\frac{\partial}{\partial r}(r u_r)\right) + \frac{\partial^2 u_r}{\partial z^2}\right] \tag{3}$$

−z-component

$$\rho\left(\frac{\partial u_z}{\partial t} + u_r\frac{\partial u_z}{\partial r} + u_z\frac{\partial u_z}{\partial z}\right) = -\frac{\partial P}{\partial z} + \mu\left[\frac{1}{r}\frac{\partial}{\partial r}\left(r\frac{\partial u_z}{\partial r}\right) + \frac{\partial^2 u_z}{\partial z^2}\right] + \rho g \tag{4}$$

−Energy Equation

$$\rho C_p\left(\frac{\partial T}{\partial t} + u_r\frac{\partial T}{\partial r} + u_z\frac{\partial T}{\partial z}\right) = k\left[\frac{1}{r}\frac{\partial}{\partial r}\left(r\frac{\partial T}{\partial r}\right) + \frac{\partial^2 T}{\partial z^2}\right] \tag{5}$$

−i-th Species Concentration Equation

$$\rho\left(\frac{\partial Y_i}{\partial t} + u_r\frac{\partial Y_i}{\partial r} + u_z\frac{\partial Y_i}{\partial z}\right) = D\left[\frac{1}{r}\frac{\partial}{\partial r}\left(r\rho\frac{\partial Y_i}{\partial r}\right) + \frac{\partial}{\partial z}\left(\rho\frac{\partial Y_i}{\partial z}\right)\right] \tag{6}$$

−State Equation

$$P = \rho R^0 T \sum_{i=1}^{3}\left(\frac{Y_i}{w_i}\right) \tag{7}$$

where Y_i and w_i are mass fraction and molecular weight of i-th species, respectively. For species concentration, the continuity equation is generally given by

$$\rho\frac{\partial Y_i}{\partial t} + \rho\vec{v}\cdot\nabla Y_i + \nabla\cdot\rho Y_i V_i = 0 \tag{8}$$

In Eq. (8), the diffusion velocities V_i which is defined by the velocity of the species with respect to

stationary coordinate axis, v_i and mass-averaged velocity, v, must be determined. This could be solved by one of the two methods: by Fick's law of mass diffusion with mass diffusivity and by the transport equation for the collection of species. In principle, while it is reasonable to use the accurate transport equation for the hydrogen mixing problem, the approximate method of Fick's law is used, as which applies on the analysis of the hydrogen combustion problems.

$$V_{ik} = -\frac{D}{Y_i}\frac{\partial Y_i}{\partial k} \tag{9}$$

where D is the mass diffusivity and Y_i is the mass fraction of i-th species. The k means the spatial coordinates (r,z).

The calculation of the mixture transport properties is carried out by approximate averaging formula recommended by Perry's Chemical Engineering Handbook[8], where the values of the properties depend on the mole fraction of each species. For each pair of gases, the mass diffusivity is calculated from the kinetic theory at given temperature and pressure:

$$D_{AB} = \frac{10^{-3}\, T^{1.75}\, [(M_A + M_B)/M_A M_B]^{1/2}}{P\, [(\Sigma_\mu)_A^{1/3} + (\Sigma_\mu)_B^{1/3}]^2} \tag{10}$$

The turbulance of mixing is treated by Prandtl's mixing length model[9] which the eddy viscosity is expressed by the gradient of local average velocity, as,

$$\nu_t = l_m^2 \left| \frac{\partial U}{\partial r} \right| \tag{11}$$

The mixing length, l_m, for a free shear flow is given as follows,

$$l_m = 0.09\,\delta \tag{12}$$

where δ is defined as the distance between points where the velocity differs from the free stream velocity by 1% of the maximum velocity. At inside of the boudary layer of subcompartment wall, a ramp function presented by Patankar ans Spalding[10] is used. On the other hand, the boundary conditions for the calculation are given as,

$$\begin{aligned} u(R,z,t) &= v(R,z,t) = 0 \\ u(r,H,t) &= v(r,H,t) = 0 \\ \frac{\partial Y_i}{\partial r}\Big|_{r=R} &= \frac{\partial Y_i}{\partial z}\Big|_{z=H} = 0 \end{aligned} \tag{13}$$

2.2. Numerical Modelling

The numerical calculation is carried out with modification of the numerical methods presented by S. V. Patankar[11]. For the governing equations shown in Section 2.1, the general equation can be established with the form,

$$\frac{\partial}{\partial t}(\rho\phi) + div(\rho \vec{u}\,\phi) = div(\Gamma\, grad\,\phi) + S \tag{14}$$

The four terms in the above equation are unsteady term, the convection term, the diffusion term, and the source term. The dependent variable ϕ can stand for a variety of different quantities, such as the mass, fraction of chemical species, the temperature, and a velocity component. Accordingly, for each of these variables, an appropriate meaning will have to be given to the diffusion coefficient Γ and the source term S. Table 3 represents the corresponding values in the governing equations.

For the cylindrical coordinate, Eq. (14) can be

Table 3. Values of ϕ , Γ, and S of Governing Equation

Equation	ϕ	Γ	S
r-direction of momentum equation	V	μ	0
z-direction of momentum equation	U	μ	ρg
Energy equation	T	k/c_p	0
Gas concentration equation	Y	D	0

expressed as,

$$\frac{\partial}{\partial t}(\rho\phi)+\frac{1}{r}\frac{\partial}{\partial r}(r\rho u\phi)+\frac{\partial}{\partial z}(\rho v\phi)$$

$$=\frac{1}{r}\frac{\partial}{\partial r}(r\Gamma\frac{\partial\phi}{\partial r})+\frac{\partial}{\partial z}(\Gamma\frac{\partial\phi}{\partial z})+S \quad (15)$$

The control volume and its grids in r-z coordinate are shown in Fig. 1. The θ-direction thickness is assumed to be unity in radian. Integrating Eq. (15) with respect to r and z over the control volume, the discretization equation is given as,

$$a_P\phi_P = a_E\phi_E + a_W\phi_W + a_N\phi_N + a_S\phi_S + b \quad (16)$$

where

$$a_P^o = \frac{\rho_P^o \Delta V}{\Delta t} \quad (17a)$$

$$b = S_C\Delta V + a_P^o\phi_P^o \quad (17b)$$

$$a_P = a_E + a_W + a_N + a_S + a_P^o - S_P\Delta V \quad (17c)$$

$$a_E = D_eA(|P_e|) + [-F_e, 0] \quad (18a)$$

$$a_W = D_wA(|P_w|) + [F_w, 0] \quad (18b)$$

$$a_N = D_nA(|P_n|) + [-F_n, 0] \quad (18c)$$

$$a_S = D_sA(|P_s|) + [F_s, 0] \quad (18d)$$

$$D_e = \frac{\Gamma_e r_e \Delta z}{(\delta r)_e}, \qquad D_w = \frac{\Gamma_w r_w \Delta z}{(\delta r)_w} \quad (19a)$$

$$D_n = \frac{\Gamma_n \frac{1}{2}(r_e + r_w)\Delta r}{(\delta z)_n}, \quad D_s = \frac{\Gamma_s \frac{1}{2}(r_e + r_w)\Delta r}{(\delta z)_s} \quad (19b)$$

$$P_e = \frac{F_e}{D_e}, \quad P_w = \frac{F_w}{D_w}, \quad P_n = \frac{F_n}{D_n}, \quad P_s = \frac{F_s}{D_s} \quad (20)$$

The symbol, [A ,B] denotes the greater of A and B. In deriving the discretization equation, the fully implicit scheme for time variable and the power-law scheme for the convection and diffusion term are used. For the equation of motion, the pressure term is included additionally and is treated by the pressure-correction equation. The flow chart for calculations is shown in Fig. 2.

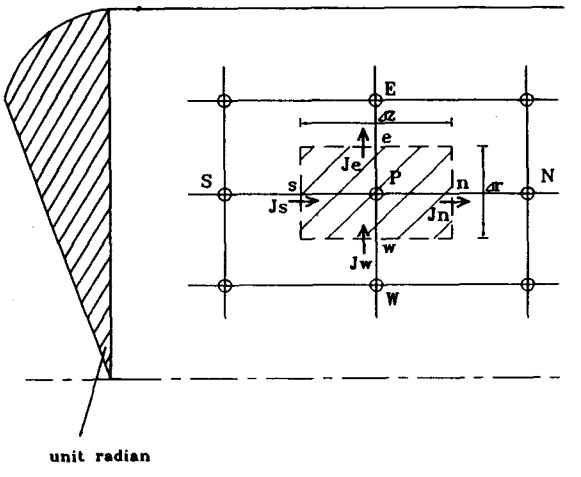

Fig. 1. Control Volume for Numerical Calculation

3. Calculation Results and Verifications

To evaluate the ability of the model to predict hydrogen mixing phenomena, experiment from Hanford Engineering Development Laboratory (HEDL) test programs has been simulated. The hydrogen mixing tests performed at HEDL are representative of events in which the hydrogen is injected at higher rates than typical values in slowly degrading core events. The tests, performed in the HEDL Containment Systems Test Facility(CSTF)[12] were intended to be representative of actual containment conditions, including the presence of steam, complex geometrical arrangements, and containment air recirculation systems. The facility and associated features are depicted in Fig. 3. The vessel is compartmentalized so that the lower region can simulate the lower compartment of an ice-condenser containment. This lower test region, which is a target of this calculation, is approximately 150 m^3 in volume and azimuthally occupies 300° of the annular region. The central core of the lower re-

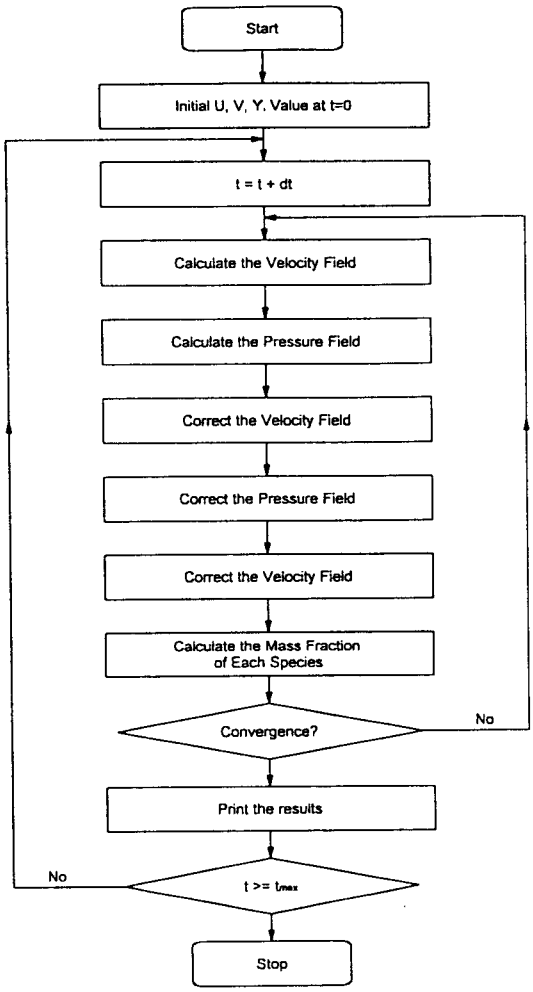

Fig. 2. Flow Chart of Numerical Calculation

gion represents the reactor cavity.

Air blowers that circulate the atmosphere from the upper to the lower region are included in the facility as shown in Fig. 3. The four air-blower openings operate at a total flow rate of 1.8 m^3/s. HEDL tests used helium as a simulant of hydrogen.

For the calculations, the following experimental conditions of the test are used.

- Helium inflow rate : 0.0067 kg/sec
- Steam inflow rate : 0.205 kg/sec.
- Compartment wall temperature : 66 ℃
- Incoming duration time of helium and steam : 600 sec.
- Recirculation flow : 104 m^3/sec

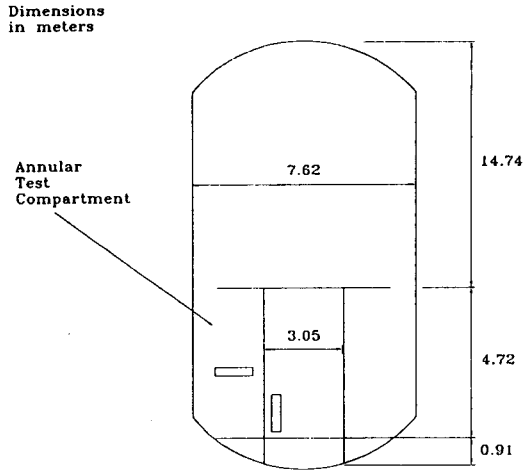

Fig. 3. Simplified HEDL Facility

Fig. 4 shows the test geometry non-uniformly nodalized, where the optimal number of nodes are investigated in 22 × 22 by preliminary runs. In Fig. 4, locations of inflow and outflow are assumed to be at middle of bottom and periphery of top of the geometry. With this nodalization the helium concentration is obtained, which compares with experimental results in Fig. 5.

The predicted peak concentration of helium shows a good agreement to experimental result over span of the calculation. But, a little discrepancies on predictions of the concentration exist; at the timing of source injection and at the final saturated stage, the higher increasing rate and the larger concentration. This results from the modelling of two-dimensionalization of test compartment.

The helium concentration is predicted to be uniformly mixed well within the compartment after the injection of sources as observed in HEDL experiments. Fig. 6 shows the degree of mixing within the compartment where the ordinate represents the concentration ratio of maximum to average values. The ratio are rapidly approaching to one when the recirculation flows start after source injection. The typi-

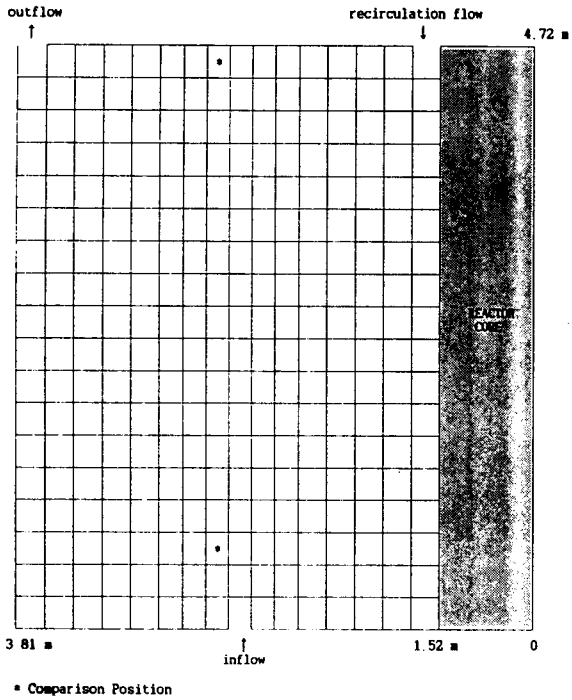

Fig. 4. The Discretization of Test Compartment

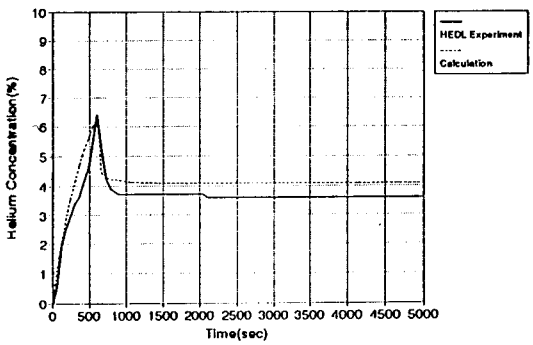

Fig. 5. The Comparison of Calculation with Experimental Result (Mixture : He-H_2O-Air)

cal of flow patterns being influenced by the recirculation flow is shown in Fig. 7, where the position of maximum helium concentration is near the source injection.

On the other hand, in this study the hydrogen mixing is simulated under the same experimental conditions in which the similar behavior is obtained as

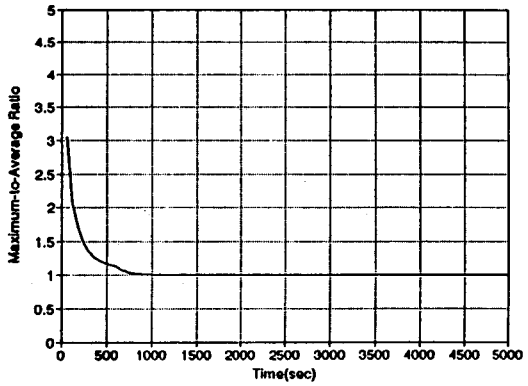

Fig. 6. Maximum-to-Average Ratio of Helium Concentration with Time

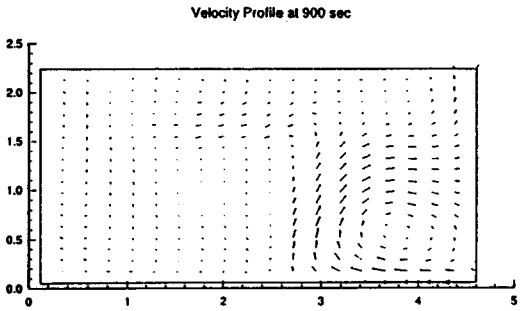

Fig. 7. Velocity Profile of Helium at 900 sec

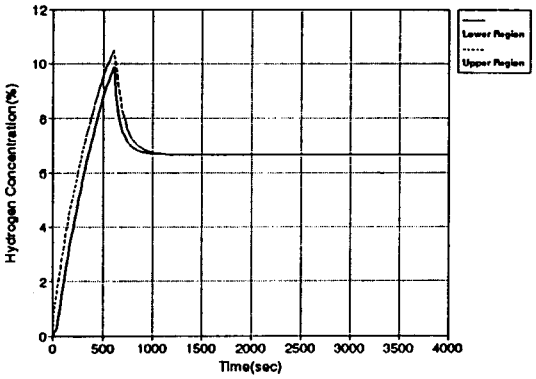

Fig. 8. Hydrogen Concentration without Obstacle (Mixture : H_2-H_2O-Air)

seen in Fig. 8. But, the concentration of the hydrogen is higher than that of the helium, since the mol-

ecular weight of the hydrogen is the smaller and the volume percent is proportional to mole concentration.

4. The Investigation of the Factors Having an Effect on the Hydrogen Mixing

Except for NUPEC hydrogen mixing experiment, any experiments to investgate the various factors having an effect on the hydrogen mixing phenomena under severe accident conditions have not been performed so far. Therefore, it is valuable to perform the qualitative assessment of hydrogen mixing using this model. In this study, the factors such as the installation of obstacles within test compartment, the variation of source injection velocity, and the variation of recirculation flow rate are investigated.

For a simulation of the source injected from the reactor cavity to the lower compartment of the containment. The test subcompartment is assumed to be similar to the HEDL Facility. The subcompartment is 5.0 m in height and from 3.0 m to 5.0 m in radius (up to 3.0 m, the reactor pressure vessel is occupied) and has 251.0 m^3 free volume. The simulant is a mixture of hydrogen-steam-air where the sources, hydrogen and steam, are continuously injected for all calculation times. If the recirculation fan operates, the timing is set to 10 minutes later from the start of calculation.

4.1. Recirculation Flow

Fig. 9 shows the average hydrogen concentrations with a obstacle of 0.2 m thick circular disk at 2.35 m in height and 1.00 m in size. Here, the term "size" means that the length from the outer subcompartment wall. Thus the size of 1.00 m corresponds to about 56% hindrance of flow area. The case (a), which simulates the simple hydrogen mixing in case of no recirculation flow, shows the concentration difference between the upper and lower region is about

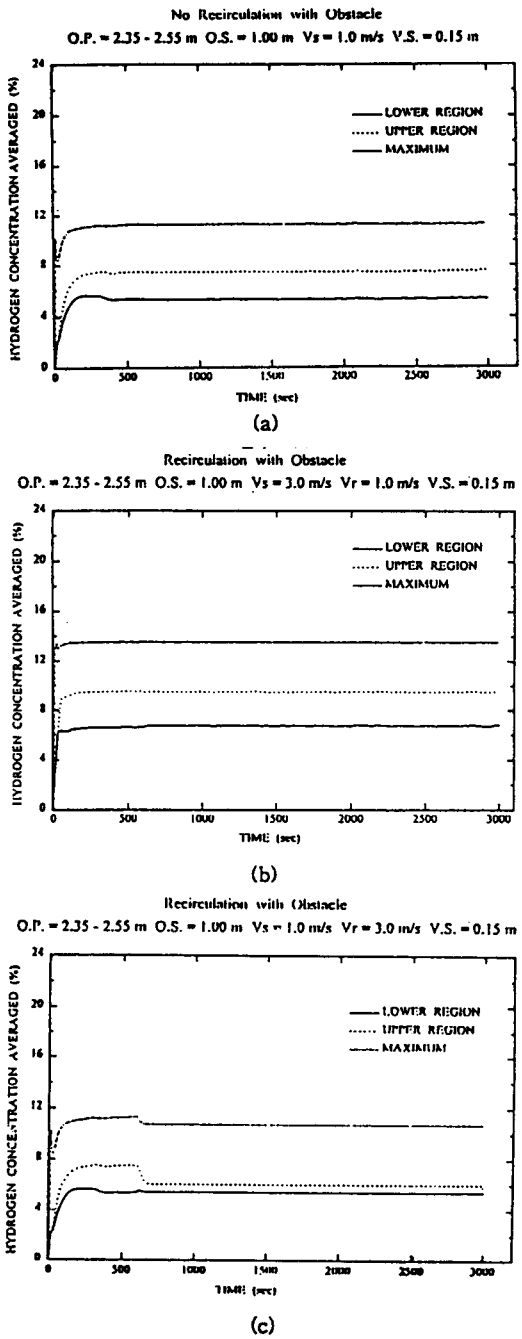

Fig. 9. The Hydrogen Concentration for the Operation of Recirculation Fan

2 %. This implies that the existence of obstacle is dominant factor in the hydrogen mixing phenomena.

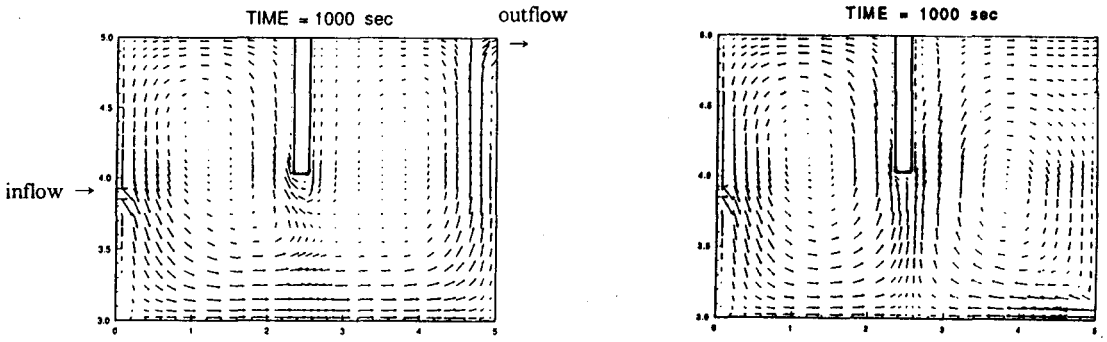

(a) No Recirculation Flow (b) Recirculation Flow

Fig. 10. The Hydrogen Velocity Profiles for the Operation of Recirculation Fan

The result of case (b) for the recirculation flow of 1.0 m/sec, is likely to be that of case (a) because the flows of source injection and recirculation go just to the opposite direction and the mass flow rate of source is larger than that of recirculation.

As seen in case (c), however, the larger the velocity of recirculation flow is the less the difference of the average concentration between the upper and lower region is. The recirculation flow can make well-mixed situation in the upper region of the subcompartment and make the momentum toward the outer wall increased. Therefore, the average concentration in the upper region is reduced.

The typical velocity profiles with and without the recirculation flow are shown in Fig. 10. For no recirculation flow, a single circulation flow pattern is formed from top and inside to bottom and outside, but partially developed. Near upper surface of obstacle, the flow is very slow. For a recirculation flow, the obstacle is a border of separated circulation fields and the flow proceeds over all region of subcompartment.

4.2. Obstacle Size

In case of no recirculation flow, the result for 0.2 m thick obstacles installed at 2.35 m in height with a size variation of 0.15 m(case a), 1.00 m(case b), and 1.50 m(case c) are shown in Fig. 11. Case (a) shows the hydrogen distribution is nearly uniform(the difference is about 0.7 %) and is similar to the mixing of free volume. But, case (b) shows the larger concentration difference of 2 %. It is stated, therefore, that the larger the size of obstacle is, the larger the concentration difference between the upper and lower region is.

But, case (c), which simulates the very small flow area from lower to upper region, shows that the concentration difference is reduced on the contrary. This unpredicted result could be explained by the fact that very severe hindrance of flow makes only a circulation of lower region and the gases penetrating the obstacle go through the upper region and exit the compartment. Hence, the hydrogen concentration of upper region is reduced and so does the concentration difference. This behavior is depicted in Fig. 12.

On the other hand, the recirculation flow makes the hydrogen distribution more complicated. Fig. 13 shows the concentration distribution for a recirculation flow of 3.0 m/sec. In case (a), the recirculation flow does proceed to the lower region and the concentration of upper region is decreased and the lower region is reversely increased. In cases of (b) and (c), the size of obstacle is so large that flows could be not formed between the upper and lower regions.

The source gases are directed to the exit along and around the obstacle peripheries. But there is a different result in cases of (b) and (c). In case (b), since the flow area is relatively small with respect to the opposite direction of the flow of source and recirculation the average concentration of the upper region is decreased. However, this phenomenon is nearly not shown in case (c) and the separated flows formed in each region makes their concentration slightly increased. It is concluded, on this point, that when the recirculation fan operates, the hydrogen concentration of region where there is a possibility of high concentration owing to the obstacle might be decreased.

4.3. Obstacle Location

The obstacle, 1.00 m in size and 0.20 m in thickness, is installed in test subcompartment. Fig. 14 shows the average concentration with a variation of obstacle location for no recirculation flow : 0.95 m (case a), 2.45 m(case b), and 3.95 m(case c). For all cases, the difference of hydrogen concentration between the upper and lower region is almost the same, but the saturated hydrogen concentration of case (c) is lower than that of other cases. Also, when the obstacle is installed close to exit, the hydrogen concentration rises its peak value, and then reaches the uniform value.

The velocity profiles for cases of (a) and (c) can easily explain the time-dependent hydrogen distribution. In low obstacle of case (a), the velocity distribution of gas does not vary to be nearly uniform the short times later. The circulation flow is not formed over all subcompartment because the gases under the obstacle make a vortex to prevent the gases going down from upper region from circulating the subcompartment. But in high obstacle of case (c), the space for flows can make a large circulation formed, and by the momentum augmented from the source the velocity of gases can be the larger and thus the hydrogen concentration reaches its peak value.

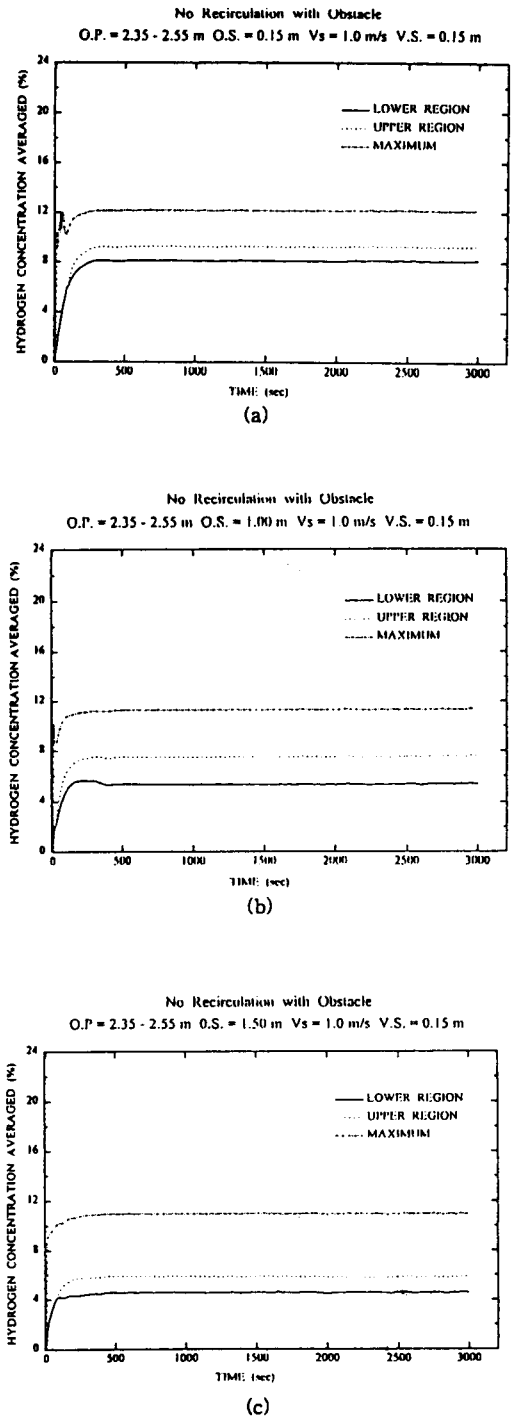

Fig. 11. The Hydrogen Concentration for the Variation of Obstacle Size without Recirculation Flow

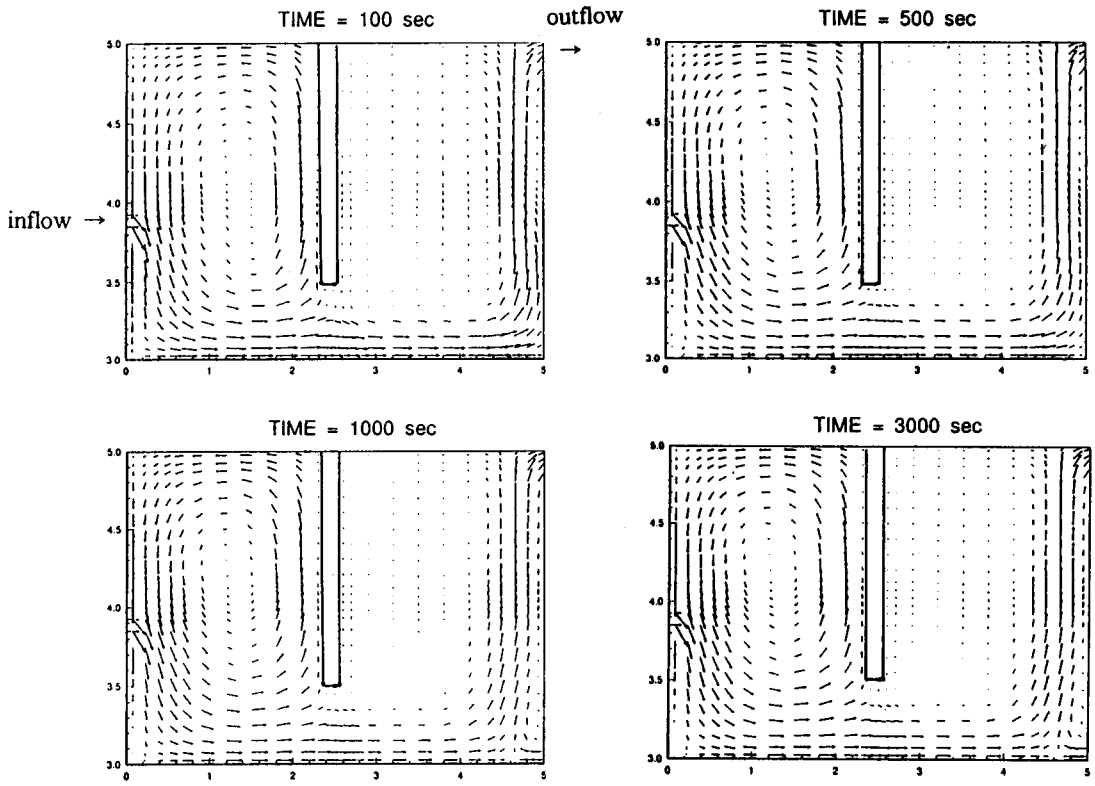

Fig. 12. The Hydrogen Velocity Profiles for the Long Obstacle without Recirculation Flow

On the other hand, for a recirculation flow, the effects of obstacle location show similar behavior like for no recirculation flow.

4.4. Source Injection Velocity

The source gases are injected at near center of subcompartment bottom with a variation of 1.0 m/sec(case a), 3.0 m/sec(case b), and 5.0 m/sec(case c). For the obstacle installed 2.45 m in height, 0.2 m in thickness, and 1.00 m in size, Fig. 15 shows the hydrogen concentration for no recirculation flow. When the mass flow rate of source increases, the average hydrogen concentration is increased from case (a) to case (c). The concentration difference between regions is increased, too. This is because the circulation flow in upper and lower region is of large separation

When the recirculation fan operates, the effects of source injection are determined by the relative velocity of source and recirculation flow. The concentration difference between regions could be decreased as shown in Fig. 16, which simulates the recirculation flow as 3.0 m/sec. Since the influxed flow into the lower region by the recirculation flow is formed, the concentration decreases in the upper region. Also, since gases recirculating from the upper region and gases injected from the source are mixed, the concentration of the lower region increases.

Therefore, it can be stated that the uniform distribution of hydrogen may be guaranteed by the recirculation flow rate comparable with source injection velocity.

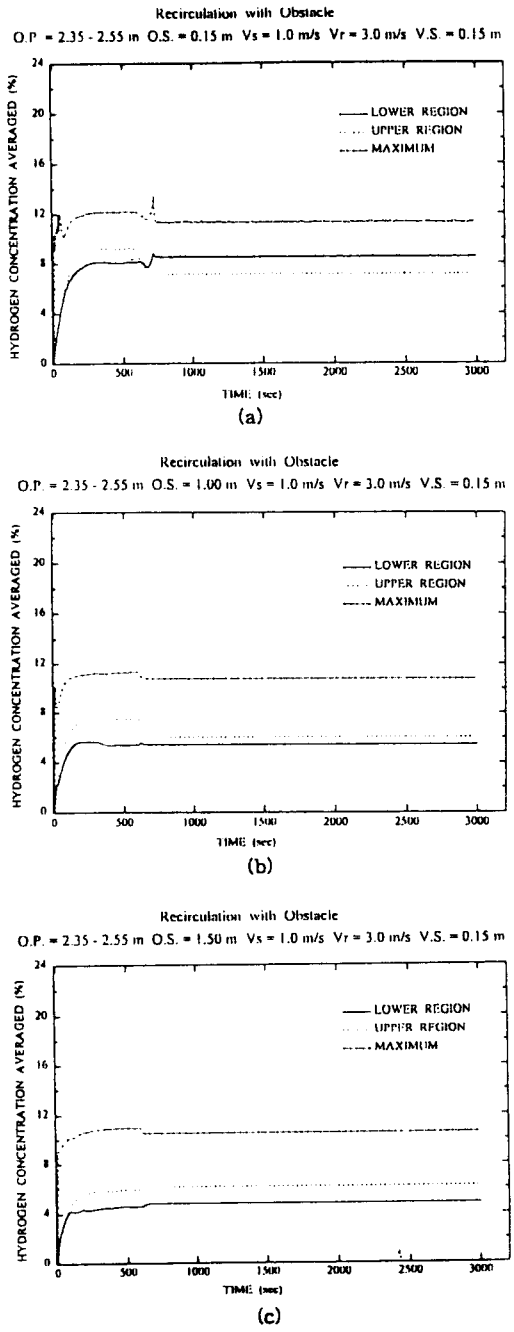

Fig. 13. The Hydrogen Concentration for the Variation of Obstacle Size with Recirculation Flow

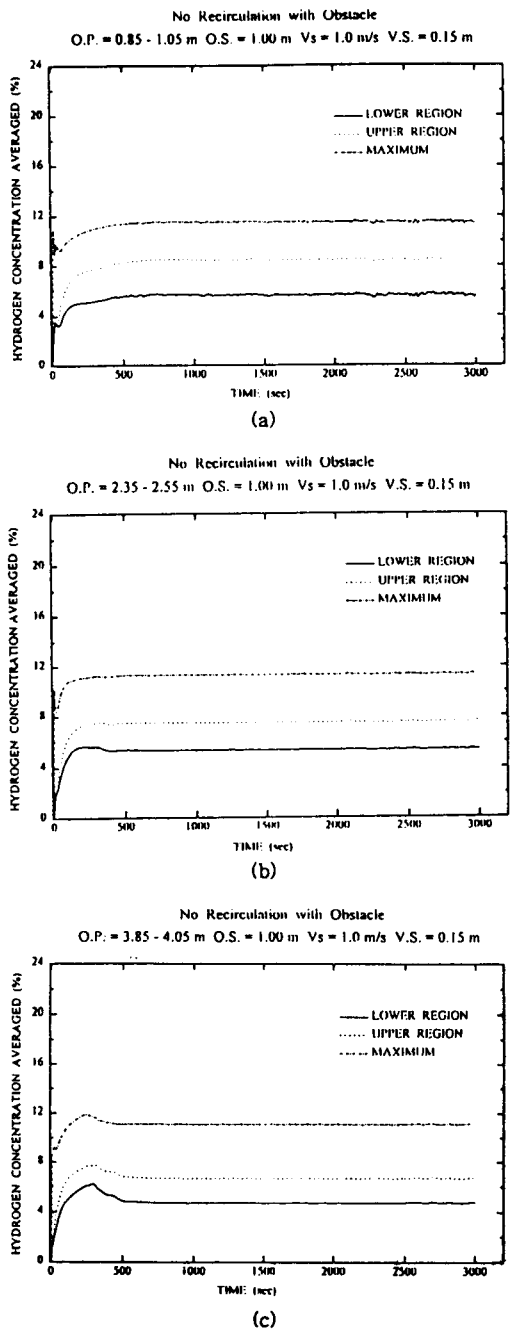

Fig. 14. The Hydrogen Concentration for the Variation of Obstacle Location without Recirculation Flow

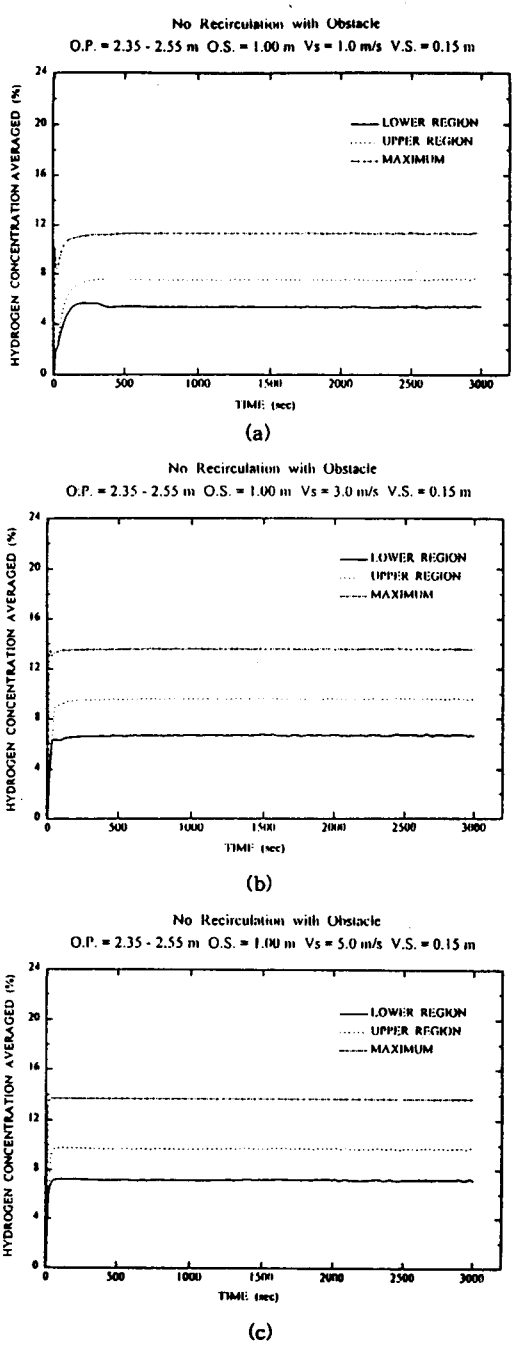

Fig. 15. The Hydrogen Concentration for the Variation of of Source Injection Velocity without Recirculation Flow

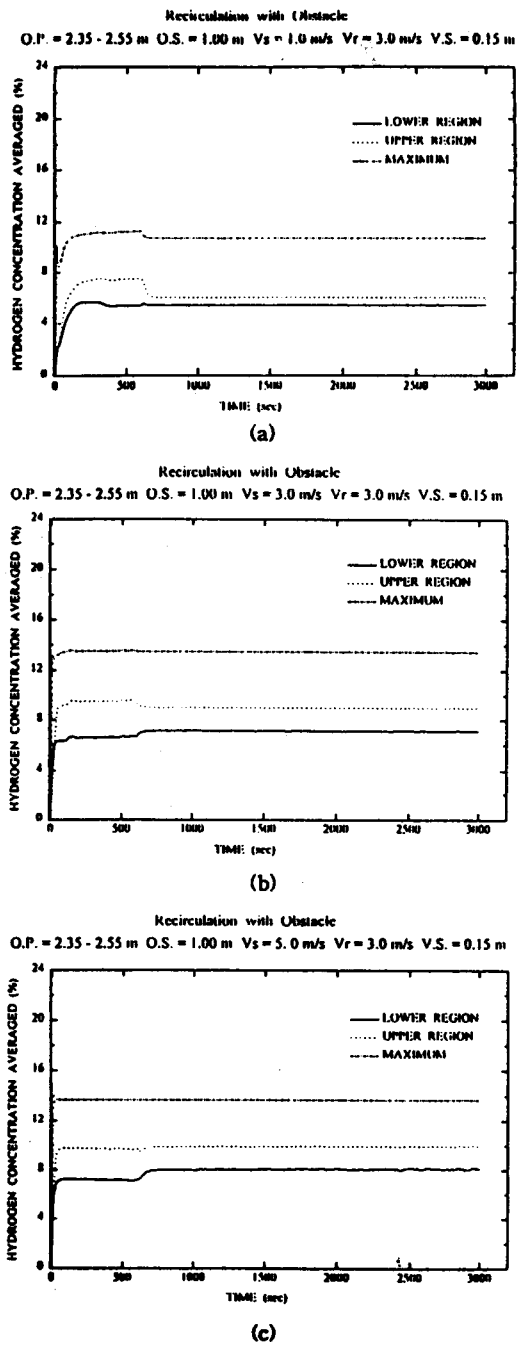

Fig. 16. The Hydrogen Concentration for the Variation of Source Injection Velocity with Recirculation Flow

5. Applied Calculations and The Generation of Supplementary Functions

From parametric studies in the previous section, the maximum-to-average ratio, which shows the extent of the nonuniform hydrogen distribution in containment subcompartment, are generated to supplement the uniform hydrogen mixing within the subcompartment predicted by lumped-parameter codes such as CONTAIN, MELCOR, and MAAP programs. This ratio can be expressed by a function of major factors having an effect on the hydrogen distribution ;

Hydrogen Distribution = f(geometrical shape of compartment, the shape of the obstacle in compartment, source injection conditions, operability of spray and/or fan, uncertainties of the prediction model, and so on) (21)

Despite of the limitation of two-dimensional model, the physical factors for the geometry configuration can make an large influence on the uniform distribution of the hydrogen within the subcompartment.

Fig. 17 is the geometry configuration for applied calculation. Fig. 17-(a) shows a simplified containment free volume, which simulates upper compartment of the reactor containment. Fig. 17-(b) shows a simplified concentric cylinder, which simulates the reactor vessel and lower compartment like a HEDL facility. The calculations of 300 cases and over are performed by considering possible combination of geometrical configuration. For each case, the calculated maximum-to-average ratio is evaluated for the generation of supplementary function, assuming that the factors behave independently one another. Four influencing factors are selected in the normalized form by considering their relative importance. The word "the importance" means that the hydrogen distribution of each case is significantly different from that of the base case. In this study, the procedure for generating the supplementary function are :

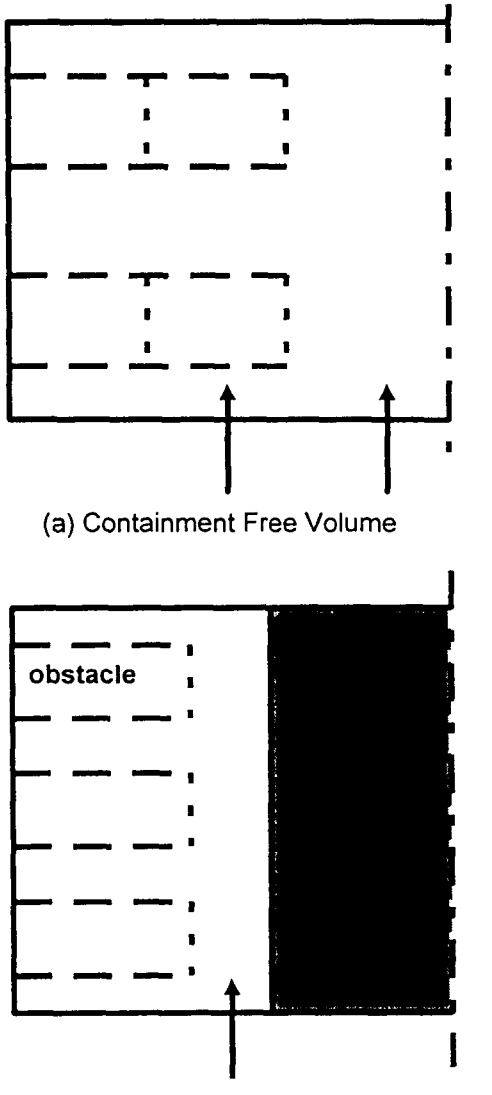

Fig. 17. The Geometry Configuration for the Generation of the Supplementary Functions

(1) group the calculation results, having a criterion of their importance.
(2) select the base case of each factor and perform the sensitivity studies.
(3) generate the basic function in each factor.
(4) determine the coefficient and its distribution of

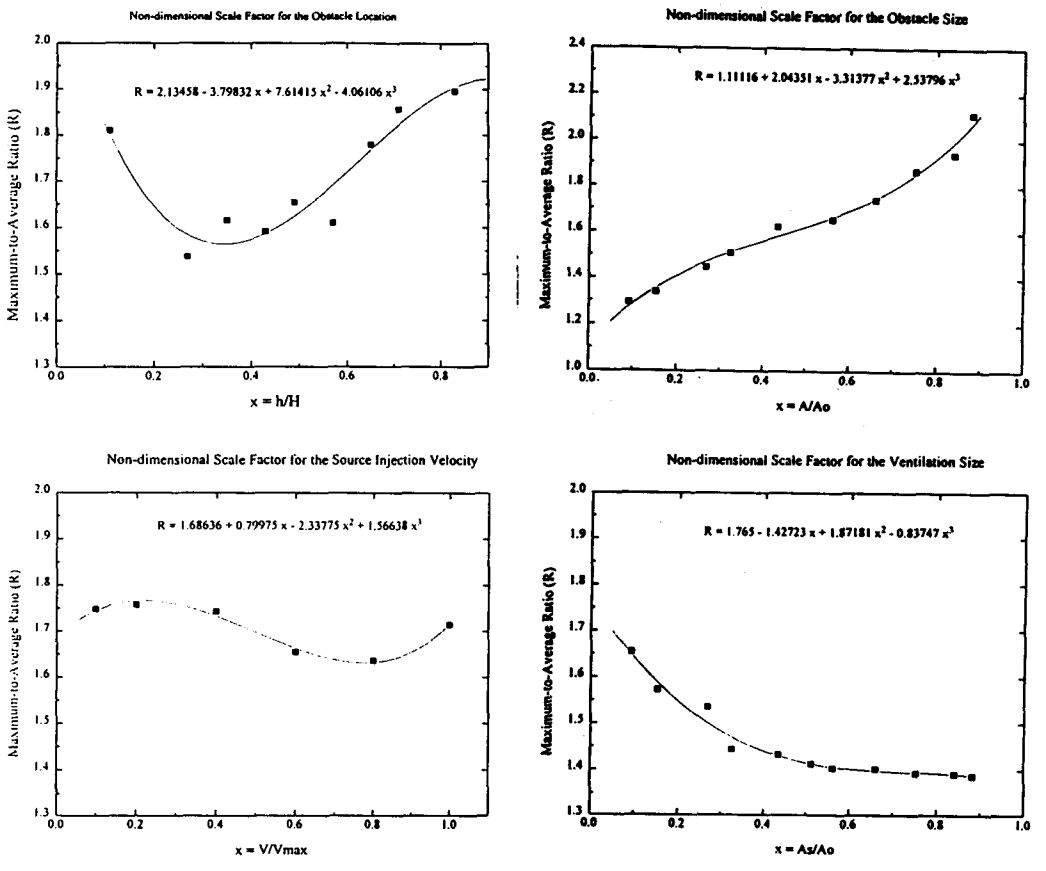

Fig. 18. The Distribution of Influencing Factors in Case of Containment Free Volume

the basic function.

(5) perform the verification test and compare this with generated supplementary function.

While some methods can be applied to generate the basic function, this study used polynomial expansion method and statistical regression method. Basic functions are obtained by interpolating the calculation results with a function of third-order polynomial, and then the overall supplementary function is generated by the regression of the distribution of each basic functions. Table 4 shows the influencing factors and the generated supplementary function. Basic functions for each factor are shown in Fig. 18.

For verification of the function several calculations under the same geometry are performed, which is shown in Table 5. The predicted results are satisfactory within the 10% of relative error. But, the generated supplementary function can only applied to a problem of the uniform concentration of the hydrogen at early time of calculation.

6. Conclusions

In this study, the hydrogen mixing model is developed to analyze the transport phenomena and predict distributions of the hydrogen concentration. Also, this study has been aimed to obtain the understanding of the qualitative mixing conditions under different geometrical and operating parameters and then a basis to establish "well-mixing" factor in the subcompartment as a supplement of lumped parameter models.

Table 4. The Generation of Supplementary Functions and Their Influencing Factors

Cases	Supplementary Functions	Value of Independent Variable
Containment Free Volume (Refer to Fig. 17-(a))	-Recirculation $R = 1.55649 + 0.56306x - 0.49854x^2 + 0.3708x^3 - 0.19768x^4$	x = geometric mean of all x_i
	-No recirculation $R = 1.68771 - 0.76850x + 1.64560x^2 - 1.1722x^3 + 0.43629x^4$	x = geometric mean of x_i (i = 1,2,3,5)
Containment Lower Compartment (Refer to Fig. 17-(b))	-Recirculation $R = 1.92024 - 1.57434x + 3.59710x^2 - 2.85255x^3 + 0.80722x^4$	x = geometric mean of all x_i
	-No recirculation $R = 1.83288 - 0.55683x - 0.82144x^2 + 3.90346x^3 - 2.52959x^4$	x = geometric mean of x_i (i = 1,2,3,5)

Influencing Factors

x_1 = non-dimensional scale factor of the obstacle location

$$= \frac{\text{height of obstacle location}}{\text{total height of the geometry}}$$

x_2 = non-dimensional scale factor of the obstacle size

$$= \frac{\text{occupied cross section of the obstacle}}{\text{total cross section of the geometry}}$$

x_3 = non-dimensional scale factor of the source injection velocity

$$= \frac{\text{injection velocity of the source}}{\text{maximum injection velocity of the source}}$$

x_4 = non-dimensional scale factor of the recirculation velocity

$$= \frac{\text{velocity of the recirculation flow}}{\text{injection velocity of the source}}$$

x_5 = non-dimensional scale factor of the ventilation size

$$= \frac{\text{occupied cross section of the outlet ventilation}}{\text{total cross section of the geometry}}$$

This model is successfully verified by comparing with selected HEDL experiments. And the dominant factors to determine the hydrogen mixing are investigated to predict the possibility of the local stratification within the subcompartment. Thus, it is concluded that

(1) nevertheless there is a limit for the simulation with two-dimensional continuum model, appropriate results are obtained.

(2) if the subcompartment has only a free volume, the hydrogen shows a well-mixed distribution and the flow is governed by the convective circulation over all subcompartment.

(3) if the obstacle disturbing the flow of gas mixture exists in the subcompartment, the uniform distribution of hydrogen may not be guaranteed.

(4) the recirculation flow must have a comparable mass flow rate relative to velocity of the source injection to sustain well-mixed conditions of the hydrogen.

Finally a functionalized supplementary factor is generated to consider the non-uniform distribution of the hydrogen in the containment subcompartment, which can be used to increase the calculation capability of lumped parameter model in design codes.

Table 5. The Comparison of Supplementary Functions with Calculation Results

Containment Free Volume			
Modes	Calculational Ratio	Functionalized Ratio	Error*
No Recirculation	1.591	1.576	−0.94
	1.479	1.588	7.37
	1.615	1.593	1.36
Recirculation	1.908	1.738	−8.91
	1.886	1.767	−6.31
	1.815	1.737	−4.30
Containment Lower Compartment			
Modes	Calculational Ratio	Functionalized Ratio	Error(%)
No Recirculation	1.651	1.713	3.76
	1.687	1.683	−0.24
	1.592	1.65	3.64
Recirculation	1.879	1.701	−9.47
	1.730	1.768	2.20
	1.739	1.715	1.38

*The error is calculated based on the calculational results

Acknowledgements

The authors acknowledge the financial and technical support provided for this work by the Korea Institute of Nuclear Safety, in particular the support of J.I. Lee, J.H. Park, and H.C. Kim.

References

1. M.J. Thurgood, "Application of COBRA-NC to Hydrogen Transport," Proc. of Second Int'l Conf. on the Impact of Hydrogen in Water Reactor Safety, NUREG/CP-0038 (1982)
2. A.L. Camp, M.J. Wester, and S.E. Dingman, "HECTR : A Computer Program for Modelling the Response to Hydrogen Burns in Containment," SAND82-1964C, NTIS (1982)
3. J.R. Travis, "HMS : A Model for Hydrogen Mitigation Studies in LWR Containments," LA-UR-8 2-2707, Los Alamos National Laboratories (1982)
4. V.P. Manno and M.W. Golay, "Analytical Modelling of Hydrogen Transport,Final Report," MIT-EL-83-009, M.I.T., NTIS (1983)
5. T. Fujimoto et al., "Development of Mixing Analysis Computer Code on Behavior of Hydrogen in Subcompartmented Containment Vessel After LOCA," Proc. of Second Int'l Conf. on the Impact of Hydrogen in Water Reactor Safety, NUREG/CP-0038 (1982).
6. H. L. Jahn, "RALOC-A New Model for the Calculation of Local Hydrogen Concentrations in Subdivided Containments Under LOCA Aspects," Proc. of Thermal Reactor Safety: Proc. of the American Nuclear Society/European Nuclear Society Topical Meeting (1980)
7. D.S. Trent and L.L. Eyler, "Application of the TEMPEST Computer Code for Simulating Hydrogen Distribution in Model Containment Structures, Proc. of the Second Int'l Topical Mtg. on Nuclear Thermalhydraulics, Vol. II, ANS (1983)
8. R.H. Perry and D. Green, "Perry's Chemical Engineers' Handbook," 6th Ed., McGraw-Hill (1984)
9. W. Rodi, "Turbulence Models and Their Application in Hydraulics- A State of the Art Review," 2nd Ed., Univ. of Karsruche, FRG (1984)
10. Patankar and Spalding, "Heat and Mass Transfer in Boundary Layers," 2nd ed. , Intertext, London (1970)
11. S.V. Patankar, "Numerical Heat Transfer and Fluid Flow," Hemisphere Publishing (1980)
12. G.R. Bloom, L.D. Muhlestein, A.K. Postma, and S.W. Claybrook, "Hydrogen Distribution in a Containment with a High Velocity Hydrogen-Steam Source," NUREG/CP-0038, 454 (1982)